CHEMICAL ENGINEERING TRANSACTIONS

VOL. 70, 2018

A publication of AIDIC

The Italian Association
of Chemical Engineering
Online at www.aidic.it/cet

Guest Editors: Timothy G. Walmsley, Petar S. Varbanov, Rongxin Su, Jiří J. Klemeš
Copyright © 2018, AIDIC Servizi S.r.l.
ISBN 978-88-95608-67-9; **ISSN** 2283-9216

DOI: 10.3303/CET1870151

Industrial Heat Pump Integration in Non-Continuous Processes Using Thermal Energy Storages as Utility – A Graphical Approach

Jan A. Stampfli[a,b,*], Martin J. Atkins[b], Donald G. Olsen[a], Beat Wellig[a], Michael R. W. Walmsley[b], James R. Neale[b]

[a]Lucerne University of Applied Sciences and Arts, Competence Center Thermal Energy Systems and Process Engineering, Technikumstrasse 21, 6048 Horw, Switzerland

[b]University of Waikato, Energy Research Center, Private Bag 3105, 7 Hamilton 3240, New Zealand

jan.stampfli@hslu.ch

The aim of this paper is to demonstrate a practical methodology for heat pump (HP) integration in non-continuous processes which is not expensive in terms of computation time and resources. Therefore, a methodology is developed based on graphical Pinch Analysis techniques and further on the developed COP Curves. The methodology is applied to an AMMIX butter production of a large dairy factory. It is shown, that by integrating a HP and using thermal energy storages (TESs) to compensate for the non-continuous behavior, the capital cost for the system is approximately reduced by the factor of 2.2. Further, greenhouse gas (GHG) emissions can be reduced with a slight decrease in total annual cost (TAC). However, by considering future natural gas and electricity prices, it is shown that the TAC can be reduced further.

1. Introduction

The reduction of greenhouse gas (GHG) emissions is a global concern for a sustainable future. In New Zealand, around 60 % of process heat is supplied by fossil fuels such as coal and gas (MBIE, 2017a). By the use of heat pumps (HPs), waste heat can be upgraded to a higher temperature level and integrated into the process to reduce heating and cooling demand and thus GHG emissions. Therefore, the industry sector is encouraged to improve the efficiency of utility systems by the integration of HPs. With processes such as pasteurization, sterilization, drying, and evaporation, HP integration in dairy industry has a high potential (Wolf et al., 2012). As an example, Walmsley et al. (2017) have integrated a hybrid compression-absorption HP to reduce the energy demand and thus GHG emissions of a milk spray dryer.

In large dairy sites, heat recovery (HR) is usually limited due to different process schedules of plants and shut down times for cleaning purposes (Atkins et al., 2009). In such processes, heating and cooling requirements will change resulting in the operating condition of the HP needing to change in time. No steady operation in the design point is possible. For a more economic operation of the HP, heat recovery loops (HRLs) combined with thermal energy storages (TESs) are used (Walmsley et al., 2013).

The challenge of HP integration in non-continuous processes is usually tackled by complex mathematical programming approaches such as by Becker (2012). Such approaches tend to be expensive concerning computation time and resources. In this paper, a practical methodology is presented using graphical techniques based on Pinch Analysis for HP integration in non-continuous processes. The methodology is based on the Time Slice Model (TSM) and uses the Grand Composite Curve (GCC) of each Time Slice (TS) for the energy targeting. Using these techniques and the introduced COP Curves, an optimal evaporation temperature for a given condensation temperature is found. Further, by using the Supply and Demand Curves of the Time Pinch Analysis (TPA) (Wang and Smith, 1995), the needed HP and the TESs sizes are determined. For demonstration purposes, the methodology is applied to an AMMIX Butter Production as a case study. Thereby, HR between an anhydrous milk fat (AMF) production plant, a cream treatment plant, and their cleaning-in-place (CIP) system

Please cite this article as: Stampfli J.A., Atkins M.J., Olsen D.G., Wellig B., Walmsley M.R.W., Neale J.R., 2018, Industrial heat pump integration in non-continuous processes using thermal energy storages as utility – a graphical approach , Chemical Engineering Transactions, 70, 901-906 DOI:10.3303/CET1870151

are analyzed and evaluated concerning CO_2e-emissions and total annual cost (TAC). The methodology in section 2 is presented by its direct application on the case study shown in section 3.

2. Methodology

2.1 Energy targets

Non-continuous processes have heating and cooling requirements which vary with time. Using the TSM, non-continuous processes are broken down into continuous sub-processes, whereby each sub-process is assigned to a TS. Based on the heat cascade, the energy targets of the individual TSs are defined.
As a result, in the case study, there are five TSs in a daily operation duration. However, just TS_2 to TS_4 have heating and cooling demand. TS_1 and TS_5 are still considered for the operation of the HP even though there are no active process streams.

2.2 COP Curves

The COP Curves are based on the Carnot cycle using a Carnot efficiency. To create the COP Curves, first, the condensation temperature for the HP system is identified by using the GCC of each TS. An overall condensation temperature on the GCC is searched, which is as close as possible to the process Pinch Temperature T_P and has a heat flow as high as possible. Condensation and evaporation temperatures are defined as

$$T_{co} = T^*_{co} + 5/4 \cdot \Delta T_{min} \tag{1}$$

$$T_{ev} = T^*_{ev} - 5/4 \cdot \Delta T_{min} \tag{2}$$

whereby two heat transfers are considered (one between HP and HRL and another one between HRL and process streams). In the case of evaporation or condensation, the temperature contributions are due to the high film heat transfer coefficient, set to $1/4 \cdot \Delta T_{min}$. In addition, for the two heat transfers of the HRLs and the one for the process streams, three temperature contributions arises, each with $1/2 \cdot \Delta T_{min}$. This results in a total shifting of 7/4 ΔT_{min}. Nevertheless, the process streams are already shifted by $1/2 \cdot \Delta T_{min}$ in the GCC and thus the total shifting of evaporation and condensation temperature results in $5/4 \cdot \Delta T_{min}$. By using the energy balance of the HP system, the emitted heat of the open type compressor is given by

$$\dot{Q}_e = \dot{Q}_a + P_{el} \cdot \eta_{drive} = \dot{Q}_a + P_i \tag{3}$$

where η_{drive} is with 0.9 the drive efficiency. Kunz et al. (2010) states that mechanical losses in reciprocating compressors are between 6-12 %. The definition of the COP is given by

$$\mathrm{COP}_{real} = \zeta \cdot \mathrm{COP}_{Carnot} = \frac{\dot{Q}_e}{P_{el}} \quad \text{with} \quad \mathrm{COP}_{Carnot} = \frac{T_{co}}{T_{co} - T_{ev}} \tag{4}$$

where ζ is the Carnot efficiency. In practice, this value is around 0.55 (Becker, 2012). To be on the save side, a value of 0.35 is chosen. For a selected condensation temperature $T^*_{co,sel}$ the resulting absorbed heat flow $\dot{Q}_a$ is determined at each possible evaporation temperature T^*_{ev}. This results in a function $\dot{Q}_a(T^*_{ev})$ with bounds at the minimal GCC temperature $T^*_{ev,min} = T^*_{GCC,min}$ and Pinch Temperature $T^*_{ev,max} = T_P$. In Figure 1, GCCs of the three relevant TSs including COP Curves (blue dotted curve, each dot is a calculated point) are shown.

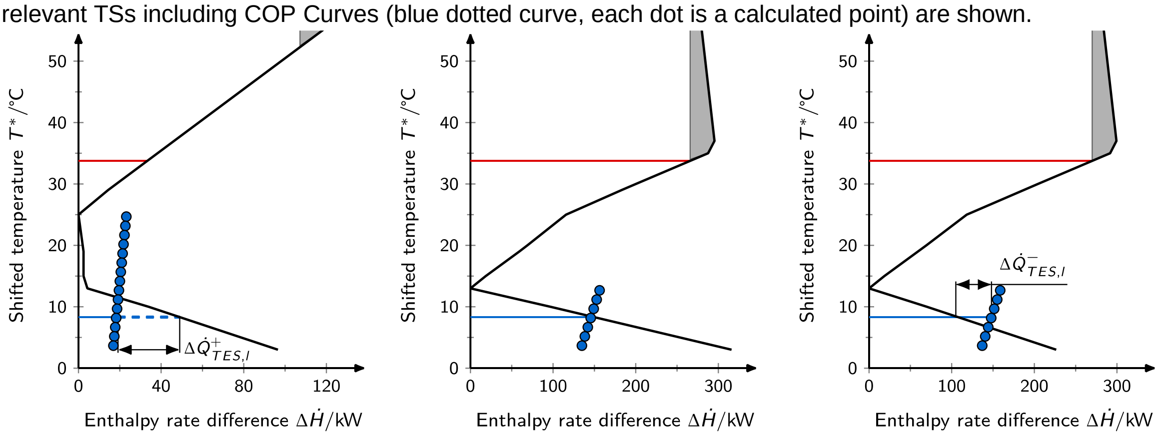

(a) GCC in TS_2 (8 – 10 h) (b) GCC in TS_3 (10 – 15.5 h) (c) GCC in TS_4 (15.5 – 17.5 h)

Figure 1: Sections of GCC of TSs including COP Curves and related absorbed and emitted heat flow of the HP. $\Delta\dot{Q}^+_{TES,I}$ represents a heat flow from the process to the TES and $\Delta\dot{Q}^-_{TES,I}$ a heat flow from the TES to the HP.

At the temperature level where the GCC and the COP Curve have an intersection, the cooling demand of the process is equal to the absorbed heat flow in the HP evaporator. For evaporation temperatures below this point, heat surplus of the process $\Delta\dot{Q}^{+}_{TES,l}$ has to be stored using TES (see Figure 1a). For evaporation temperatures above the intersection, heat deficit of the process $\Delta\dot{Q}^{-}_{TES,l}$ has to be provided by TES (see Figure 1c). The optimal evaporation temperature $T^{*}_{ev,opt}$ is found at the point where the sum of the heat surpluses and deficits overall TSs (l=1…5) is equal to zero which is given by

$$\sum_{l=1}^{L} \Delta\dot{Q}^{\pm}_{TES,l}\left(T^{*}_{ev.opt}\right) \cdot \Delta t_l = \sum_{l=1}^{L} \dot{Q}_{a,l}\left(T^{*}_{ev,opt}\right) \cdot \Delta t_l - \sum_{l=L}^{L} \Delta\dot{H}_{GCC,l}\left(T^{*}_{ev,opt}\right) \cdot \Delta t_l = 0 \tag{5}$$

where Δt_l represents the TS duration. For the case study, a condensation temperature of $T^{*}_{co,sel}$ = 33.67 °C is selected which results in an optimal evaporation temperature of $T^{*}_{ev,opt}$ = 7.94 °C. By introducing the $HR,T^{*}_{ev,opt}$ -diagram in Figure 2, the optimal condensation temperature is found graphically as well.

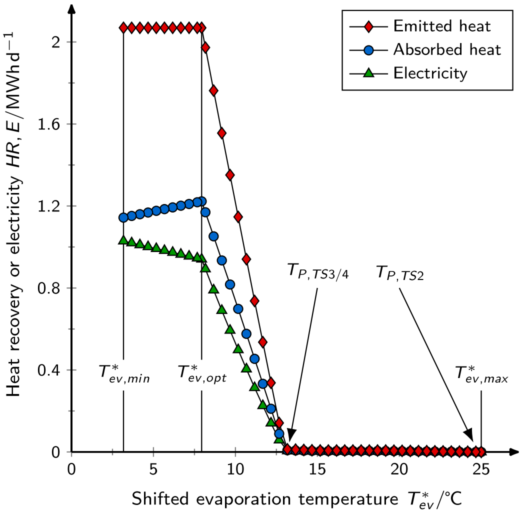

Figure 2: HR due to HP integration as a function of the shifted evaporation temperature for a given condensation temperature of 33.76 °C.

2.3 Supply and Demand Curves

The principles of the Supply and Demand Curves (Wang and Smith, 1995) which is used for utility system sizing, are visualized in a $\Delta Q,t$-diagram in Figure 3, whereby transferred heat from or to a process stream in relation to time is plotted. For the HP integration, two Supply and Demand Curves are plotted, one for the emitted heat of the HP (Figure 3a) and one for the absorbed heat of the HP (Figure 3b).

The highest demand for the HP occurs with 270 kW emitted and 160 kW absorbed heat flow in TS_4. If there is no storage, the HP has to be designed for this TS. By introducing a storage for the emitted heat with 1,350 kWh and one for the absorbed heat with 800 kWh, the needed heat flows can be reduced to 86 kW emitted and 51 kW absorbed. Thereby, the HP is able to operate continuously for 24 h/d. By using the temperature constraints and the density of the HRL/storage media, an overall HP-TES system can be determined as shown in Figure 4.

2.4 Evaluation of economics and emissions

To evaluate the integration of the HP-TES system, the TAC is estimated by

$$\mathrm{TAC} = \frac{i\,(1+i)^n}{(1+i)^n-1} \cdot \sum_E \left(F_E \cdot \frac{\mathrm{I_{PMEI2}}}{\mathrm{I_{PMEI1}}} \cdot \mathrm{MPIC}_E\right) + C_{op,a} \quad \text{with} \quad \mathrm{MPIC}_E = C_{E,0} + C_{E,1}\, Q^{f_{E,d,1}} + C_{E,2}\, Q^{f_{E,d,2}} \tag{7}$$

Where i is the interest rate, and n is the investment period. The equipment cost is estimated using factorial methods. To calculate the capital cost of equipment, main plant item cost (MPIC) is multiplied by Lang factors F_E (Lang, 1948), where installation, piping, control system, building, site preparation, and service facility cost is included. To consider inflation and deflation, the cost function is corrected using the plant, machinery, equipment group index (I_{PMEI}) of capital goods price index (CGPI) (Stats NZ, 2017). Q is the capacity of the equipment. The annual operating cost is estimated by

$$C_{op,a} = Q_{HU} \cdot c_{HU} + Q_{CU} \cdot c_{CU} + E_{el} \cdot c_{el} \tag{8}$$

where Q represents the utility and E the electricity demand per year. The specific energy cost c also includes the cost for CO_2e-emissions. The annual CO_2e-emissions are given by

$$\mathrm{CO_2e} = Q_{HU} \cdot \xi_{HU} + Q_{CU} \cdot \xi_{CU} + E_{el} \cdot \xi_{el} \tag{9}$$

where ξ is the corresponding specific CO_2e-emission in t_{CO2e}/MWh.

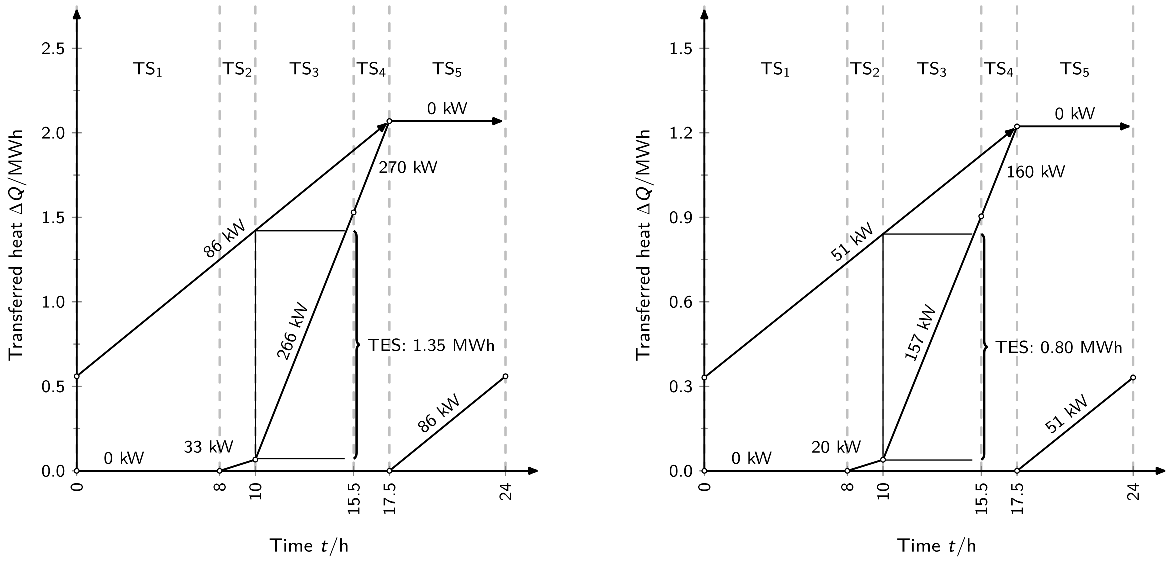

(a) Emitted heat at T_{co} = 46.26 °C (b) Absorbed heat at T_{ev} = -4.56 °C

Figure 3: HP Supply and Demand Curves in ΔQ,t-diagram for optimum sizing of HP-TES system.

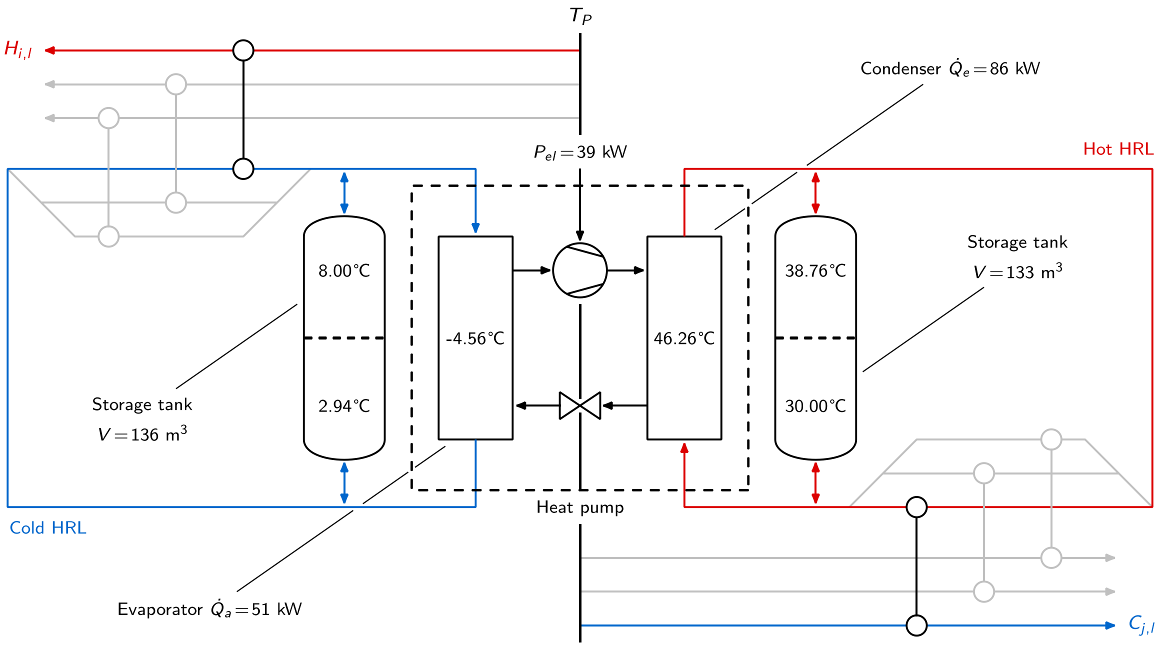

Figure 4: Resulting HP-TES system.

3. Dairy factory case study

The graphical methodology is applied to a large dairy factory as a case study. Thereby, HR between an AMF production plant, a cream treatment plant, and their CIP system are analyzed. Due to the different schedules of the plants, the heating and cooling demand is changing over time. The stream data is provided in Table 1. Table 2 summarizes the cost function coefficients for the used equipment and the utility data is provided in Table 3. Further, an investment period n = 12 y and an interest rate i = 7 % is given.

Table 1: Stream data for the case study

Stream	T_S (°C)	T_T (°C)	CP (kW/K)	$\Delta\dot{H}$ (kW)	h (W/(m^{2}K))	t_{start} (h)	t_{end} (h)
AMF production							
Cream heating	8	68	32.54	1952.4	500	10	17.5
Oil past.	68	95	11.83	319.4	500	10	17.5
AMF cooling	95	40	13.64	750.2	500	10	17.5
Buttermilk therm.	68	80	13.95	167.4	500	10	17.5
Buttermilk cooling	80	8	13.95	1004.4	500	10	17.5
Beta Serum cooling	68	8	8.42	505.2	500	10	17.5
Wash Water heating	20	90	3.47	260.3	2,000	10	17.5
Polish Waste cooling	90	42	4.7	225.6	500	10	17.5
Deodorizer evap.	25	177.67	0.27	155.5	5,000	10	17.5
Deodorizer cond.	177.67	25	0.41	234.0	5,000	10	17.5
Cream treatment							
Cream past.	8	88	8.95	716	500	8	15.5
Trd. cream cooling	88	8	8.95	716	500	8	15.5
SCC evap.	24	177.67	0.41	234.4	5,000	8	15.5
SCC cond.	177.67	24	0.41	234.4	5,000	8	15.5
CIP system							
Pre rinse water	20	50	0.92	27.6	2,000	8	17.5
Alkaline solution	20	75	1.84	101.2	2,000	8	17.5
Nitric acid	20	50	1.23	61.5	2,000	8	17.5
Post rinse water	20	15	0.92	4.6	2,000	8	17.5

Table 2: Equipment cost coefficients with an uncertainty of ±30 % (provided by Bouman et al. (2005) and Stats NZ (2017)).

Equipment	Q (-)	C_0 (NZD)	C_1 (NZD)	$f_{d,1}$ (-)	C_2 (NZD)	$f_{d,1}$ (-)
Stainless steel plate HEX	A (m^2)	4,350	660	1	-	-
Reciprocal piston compressor	P_i (kW)	42,280	5,940	1	4,090	2
Variable speed drive motor	P_{el} (kW)	4,020	490	1	-	-
Storage vessel	V (m^3)	-	1,530	0.597	-	-
Refrigeration unit	$\dot{Q}_n$ (kW)	-	11,320	0.806	-	-
Natural gas steam boiler	$\dot{Q}_m$ (kW)	-	1,060	0.805	-	-
Natural gas water boiler	$\dot{Q}_m$ (kW)	13,210	0,140	1	-	-

Table 3: Utility data for the case study (provided by MBIE (2017b), Em6 (2017), and EECA (2017))

Utility	T_S (°C)	T_T (°C)	h (W/(m^{2}K))	c_{day} (NZD/MWh)	c_{night} (NZD/MWh)	ξ (t_{CO2e}/MWh)
Steam	190	190	5,000	54.2	54.2	0.21
Hot water	100	95	2,000	54.2	54.2	0.21
Chilled water	-5	0	2,000	34.8	27.8	0.04
Electricity	-	-	-	102.6	82.6	0.13

4. Results and discussion

In Table 4 it is shown, that the capital cost for the HP system by integration of two TESs is approximately reduced by the factor of 2.2. By the integration of the HP-TES system in the case study, the HU demand is reduced from 1,900 MWh/y to 1,196 MWh/y and the CU demand from 885 MWh/y to 522 MWh/y. As a result, the CO_2e-emissions are reduced from 434 t_{CO2}/y to 317 t_{CO2}/y. Thereby, additional electricity of 379 MWh/y is needed. The TAC is slightly decreased from 431,168 NZD/y to 422,169 NZD/y. By analyzing predicted future natural gas and electricity prices from 2050 (90 NZD/MWh_{NG}, 130 NZD/MWh_{el}, MBIE, 2016), the integration of an HP reduces the TAC further from 529,399 NZD/y to 495,583 NZD/y.

Table 4: Comparison of HP system with and without TES

Equipment	Capacity unit	Capacity ([Q])		Capital cost (NZD)	
		HP with TES	HP without TES	HP with TES	HP without TES
Compressor	P_i (kW)	35	122	256,829	672,848
Motor	P_{el} (kW)	39	135	23,218	70,259
Evaporator	A (m^2)	3.4	11	6,589	11,458
Condenser	A (m^2)	5.3	17	7,877	15,399
Cold TES	V (m^3)	136	-	28,807	-
Hot TES	V (m^3)	133	-	28,359	-
Total capital cost				351,679	769,964

5. Conclusions

By the use of TES beside the HP, capital cost for the system are more than halved. Further, by the application of the developed COP Curves and the Supply and Demand Curves, an HP-TES system can be integrated beneficial in terms of GHG emissions and TAC which is slightly decreased. By analyzing future natural gas and electricity prices, it is predicted, that the HP-TES integration will be more economic in future.

The resulting temperature differences in the condenser and evaporator are too high compare to practical applications. To improve this, a mathematical programming approach should be performed to adjust condenser, evaporator, and storage temperature levels by minimization of TAC.

Acknowledgments

This research project is financially supported by the Swiss Innovation Agency Innosuisse and is part of the Swiss Competence Center for Energy Research SCCER EIP.

References

Atkins M.J., Walmsley M.R.W., Neale J.R., 2009, The challenge of integrating non-continuous processes – milk powder plant case study, Chemical Engineering Transactions, 18, 445-450.

Becker H.C., 2012, Methodology and thermo-economic optimization for integration of industrial heat pumps, PhD Thesis, École Polytechnique Féderale de Lausanne Département de Génie Mécanique, CH.

Bouman R.W., Jesen S.B., Wake M.L., 2005, Process capital cost estimation for New Zealand 2004, Society of Chemical Engineers New Zealand.

EECA (Energy Efficiency and Conservation Authority), 2017, CO2 emission calculator <www.eecabusiness .govt.nz /tools/wood-energy-calculators/ co2-emission-calculator/> accessed 21.11.17.

Em6, 2017, Electricity market overview < www.em6live.co.nz.> accessed 20.11.17.

Kunz R., Winkelmann B., Mokhatab S., 2010, Efficiency and operating characteristics of centrifugal and reciprocating compressors, Pipeline & Gas Journal, 237(10), 42-46.

Lang H.J., 1948, Simplified approach to preliminary cost estimates, Chemical Engineering, 55(6), 112-113.

MBIE (Ministry of Business, Innovation and Employment, New Zealand), 2017a, New Zealand energy efficiency and conservation strategy 2017-2022.

MBIE (Ministry of Business, Innovation and Employment, New Zealand), 2017b, Energy in New Zealand 2017 <www.mbie.govt.nz/info-services/sectors-industries/energy/energy-data-modelling/publications/energy-in-new-zealand.> accessed 20.11.17.

MBIE (Ministry of Business, Innovation and Employment, New Zealand), 2016, Electricity demand and generation scenarios results. <mbienz.shinyapps.io/edgs-results-app/> accessed 19.12.17

Stats NZ, 2017, Price index by item – plant, machinery and equipment <www.stats.govt.nz/infoshare/> accessed 20.11.2017.

Walmsley T.G., Klemeš J.J., Walmsley M.R.W., Atkins M.J., Varbanov P.S., 2017, Innovative hybrid heat pump for dryer process integration, Chemical Engineering Transactions, 57, 1039-1044.

Walmsley M.R.W., Atkins M.J., Walmsley T.G., 2013, Application of heat recovery loops to semicontinuous processes for process integration, In Klemeš J.J. (Ed), 2013, Handbook of Process Integration (PI): Minimisation of Energy and Water Use, Waste and Emissions, Woodhead Publishing Limited, 594-627, Cambridge, UK.

Wang Y.P., Smith R., 1995, Time Pinch Analysis, Chemical Engineering Research & Design, 73(8), 905-914.

Wolf S., Lambauer J., Blesl M., Fahl U., Voss A., 2012, Industrial heat pumps in Germany: Potentials, technological development and market barriers. In ECEEE 2012 summer study – energy efficiency in industry, 543-550.